Dissociating Excitons Photogenerated in Semiconducting Carbon Nanotubes at Polymeric Photovoltaic Heterojunction Interfaces

Dominick J. Bindl, Nathaniel S. Safron, and Michael S. Arnold*

Department of Materials Science and Engineering, University of Wisconsin, Madison, Wisconsin 53706, United States

ABSTRACT Semiconducting single-walled carbon nanotubes (s-SWCNTs) have strong near-infrared and visible absorptivity and exceptional charge transport characteristics, rendering them highly attractive semiconductor absorbers for photovoltaic and photodetector technologies. However, these applications are limited by a poor understanding of how photogenerated charges, which are bound as excitons in s-SWCNTs, can be dissociated in large-area solid-state devices. Here, we measure the dissociation of excitons in s-SWCNT thin films that form planar heterojunction interfaces with polymeric photovoltaic materials using an exciton dissociation-sensitive photocapacitor measurement technique that is advantageously insensitive to optically induced thermal photoconductive effects. We find that fullerene and polythiophene derivatives induce exciton dissociation, resulting in electron and hole transfer, respectively, away from optically excited s-SWCNTs. Significantly weaker or no charge transfer is observed using wider gap polymers due to insufficient energy offsets. These results are expected to critically guide the development of thin film s-SWCNT-based photosensitive devices.

KEYWORDS: carbon nanotube · exciton · dissociation · photocapacitor · photovoltaic

Semiconducting single-walled carbon nanotubes (s-SWCNTs) have remarkable optoelectronic properties such as band gap tunability,[1] strong optical absorptivity,[2] ultrafast charge transport mobility,[3] solution-processability, and excellent chemical stability.[4] Overall, the outstanding properties of these semiconductors make them highly attractive absorbers for next-generation photovoltaic and photodetector applications.[4]

The optical band gap, E_g, of s-SWCNTs can be tuned to optimize absorption of different spectral ranges by tailoring the distribution of their diameters, d. For example, efficient absorption of the solar spectrum can be achieved by tuning $d = 7-12$ Å resulting in $E_g = 1.0-1.3$ eV,[1,4] near the Shockley−Queisser optimum for a single-junction photovoltaic device. Alternatively, $E_g < 1.0$ eV can be achieved enabling absorption deeper into the infrared for photodetector applications by tuning $d > 12$ Å. In addition to band gap tunability, thin films of s-SWCNTs have strong optical absorptivity $\alpha > 10^5$ cm^{-1} at their band gap,[2,4] allowing for the collection of incident radiation in films as thin as 100 nm. Recent measurements of multiple exciton generation in carbon nanotube transistors[5] suggest photovoltaic efficiencies in excess of the Shockley−Quiesser limit may potentially be achieved with s-SWCNT-based devices. Furthermore, the mobility of free charges in s-SWCNTs exceeds 10^4 cm^2 V^{-1} s^{-1}, facilitating the collection of photogenerated charges once they are separated.[3,4] Additionally, recent advances in the sorting of SWCNTs have provided access to the properties of s-SWCNTs with negligible presence of metallic SWCNTs, which are anticipated to compromise the performance of s-SWCNT-based devices.[6]

Overall, the outstanding properties of s-SWCNTs render them highly attractive semiconductor absorbers for next-generation photovoltaic and photodetector applications. However, one challenge that still impedes the development of s-SWCNT-based devices is that electron−hole pairs photogenerated in s-SWCNTs are bound as excitons.[7] The exciton binding energy, E_B, significantly exceeds room temperature thermal energy k_BT, and as a result, the spontaneous separation of photogenerated charges in s-SWCNTs is not efficient without an external mechanism to drive their dissociation.

Previously, exciton dissociation has been accomplished in individual s-SWCNT field effect transistors and p−n junctions *via* a field-dissociation mechanism.[8,9] In such devices, dissociation occurs in strong fields arising from band bending near metal−nanotube Schottky contacts or due

*Address correspondence to msarnold@wisc.edu.

Received for review June 2, 2010 and accepted September 27, 2010.

Published online October 5, 2010.
10.1021/nn1012397

to split gate biasing.[5,10] While individual s-SWCNT devices have invaluably aided in understanding nanotube photophysics, the absolute absorbance of a single nanotube is insufficient for large-area photovoltaic and photodetector applications. In contrast, large-area films of *many* nanotubes with an optical density ~1 are needed to more realistically implement s-SWCNTs as the optically absorptive components of photosensitive devices.

In thin films, the dissociation of excitons in s-SWCNTs can be accomplished through the formation of a staggered gap donor/acceptor, type-II heterojunction between the s-SWCNTs and a second semiconductor in which the energy offsets at the heterointerface exceed E_B. In this scenario, exciton dissociation at the interface results in charge transfer from the s-SWCNTs to the second semiconductor. The separated charges on opposite sides of the interface have different chemical potentials and can be harvested for photovoltaic energy conversion or used to generate a current for photodetector applications.

Here, the question we have sought to answer is: What materials commonly utilized in polymer photovoltaic devices have the appropriate energetics to form a staggered gap donor/acceptor type-II heterojunction with s-SWCNTs with sufficient energy offsets to achieve exciton dissociation and charge separation in thin films? Prior measurements of photogenerated charge separation in complexes between s-SWCNTs and polymers or molecules *in solution* do not necessarily translate to solid-state thin films due to differences in the polarizability and the local environment that immediately surround the s-SWCNTs, affecting charge screening and E_B.[11] In thin films, the experimental characterization of charge separation at nanotube/semiconductor interfaces has been confounded by two effects. First, the prevalence of m-SWCNTs in as-produced nanotube material has been problematic because m-SWCNTs rapidly quench excitons in films. Second, the optical excitation of nanotube thin films is known to induce a photoconductivity that arises from thermal effects, independent of exciton dissociation.[12] As a result, the materials pairings necessary to achieve s-SWCNT exciton dissociation and charge separation in s-SWCNT thin films are poorly understood.

Here, we have studied exciton dissociation at s-SWCNT/semiconductor heterojunction interfaces in thin films using a novel photosensitive capacitor measurement technique that can sensitively measure charge transfer away from optically excited s-SWCNTs to the semiconductor. Because this technique measures the buildup of separated charge rather than a photoconductivity, it is advantageously insensitive to photothermal induced changes in conductivity that have plagued previous thin film measurements. Additionally, we have implemented postsynthetically sorted s-SWCNTs in our studies rather than mixed as-produced nanotubes in order to more clearly characterize the conditions necessary to achieve exciton dissociation in the semiconducting tubes without the effects of neighboring metallic tubes. Our work is unique from previous investigations of nanotubes in photovoltaic devices[13−16] where nanotubes have fulfilled secondary roles, for example, as electrode materials or as materials for accepting, transporting, and collecting charge. In contrast, here, we are specifically seeking to learn how to exploit carbon nanotubes at the center of photovoltaic device functionality, specifically as semiconductor optical absorbers.

We have specifically examined exciton dissociation and charge transfer at s-SWCNT heterojunction interfaces with archetypical polymeric photovoltaic materials including fullerenes, poly(thiophene)s, poly(phenylene vinylene)s, and poly(fluorene)s. These polymeric photovoltaic materials can be easily incorporated into device stacks with s-SWCNTs *via* solution-processing or vacuum thermal evaporation. Additionally, the energy levels of these materials have been well-characterized in literature, which facilitates the prediction of which materials should form type-II heterojunction with s-SWCNTs. We have also characterized s-SWCNT/polycarbonate heterojunctions for comparison with the findings of Pradhan et al.,[17] who have suggested that exciton dissociation and charge transfer occur between the two materials.

In the photoactive capacitors, planar thin-film s-SWCNT/semiconductor heterojunctions are sandwiched between a transparent conducting anode and an insulating polymer film that is capped by a metallic cathode. The role of the insulating polymer film is to act as the dielectric of the photosensitive capacitor that charges when there is an exciton dissociation-generated photocurrent. The technique avoids misleading thermally induced photoconductive effects because a direct current does not flow through the capacitor device.

To measure exciton dissociation using the capacitors, a time-modulated exciton population is generated on the s-SWCNTs using a spectrally resolved time-modulated light source. In the absence of a driving force for dissociation, excitons photogenerated on s-SWCNTs recombine without separation and a charge buildup on the capacitor is not detected. In contrast, charge will build up on the capacitor if there is electron or hole transfer from the photoexcited s-SWCNTs to the donor or acceptor materials. In this case, charge evolution and buildup can be quantified by either measuring the transient photovoltage on the capacitor or by characterizing the transient charging and discharging current in response to the pulsed illumination.

RESULTS AND DISCUSSION

High-quality s-SWCNTs were prepared from powders of SWCNTs grown by a high-pressure carbon monoxide conversion (HiPCO) process, purchased unpuri-

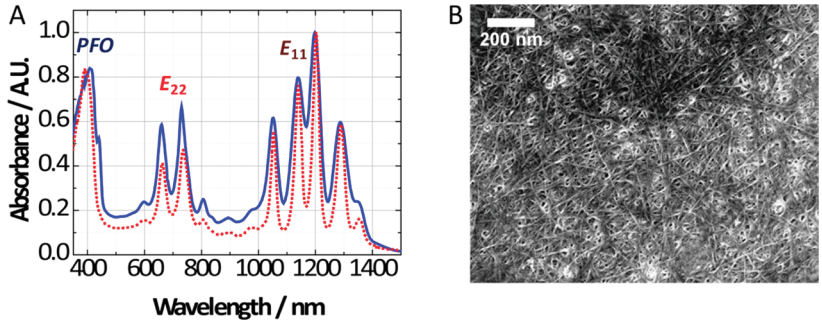

Figure 1. (A) Normalized optical absorptivity of PFO-wrapped s-SWCNTs in chloroform solution (dotted, red) and in thin films (solid, blue). (B) SEM micrograph of a thin film of 1:1 PFO:s-SWCNTs on ITO coated glass.

fied from Unidym (d = 8−12 Å.) Isolation of semiconducting species from polydisperse, electronically heterogeneous as-produced HiPCO powder was achieved through a procedure similar to that of Nish et al.,[18] selectively solubilizing s-SWCNTs through a wrapping interaction between high chiral angle s-SWCNTs and poly(9,9-dioctylfluorene-2,7-diyl) (PFO). Excess PFO was removed from the dispersions *via* several iterations of differential s-SWCNT sedimentation (Figure 1a). The E_{22} optical cross-section-full width half max product of Tsyboulski et al.[2] (8.4×10^7 nm cm^2 mol^{-1}) was used to determine the s-SWCNT concentration considering the (8,6), (7,6), (7,5), (8,7), and (9,7) chiralities,[19] and it was determined that the final s-SWCNT solutions had a PFO:s-SWCNT mass-ratio tunable from 4:1 to 1:1, depending on the specific solvent used for PFO removal. Absorption due to spurious metallic nanotubes in the range of 450−600 nm was not detected, indicating the high purity of the semiconducting species.

To fabricate the photosensitive capacitors, planar thin films of s-SWCNTs (~7 nm) were cast onto the transparent anode (indium−tin oxide, ITO) *via* a doctor-blading technique. A scanning electron micrograph demonstrates a doctor-bladed film of PFO wrapped s-SWCNT (Figure 1B) with a 1:1 weight ratio of PFO:s-SWCNT. The s-SWCNT remain well isolated, as determined from the persistence of sharp E_{11} and E_{22} absorption peaks in the films (Figure 1A). The root-mean-square (rms) roughness of the films was 4.4 nm as compared to 2.2 nm for bare ITO (Figure S1, Supporting Information).

Following the deposition of the s-SWCNTs, thin films of the polymeric photovoltaic materials were deposited on top of the s-SWCNTs by either vacuum thermal evaporation or spin-casting from solution to form the planar heterojunctions. Poly(vinylpyrrolidone) (PVP) dielectric films (2.0 ± 0.5 um) were then spun-cast atop the heterojunctions from a methanol solution and 50 nm Ag was evaporated for the cathode. Two subsets of active interfaces were fabricated, one which was annealed at 130 °C both before and after dielectric deposition, and one which was not annealed at all.

A schematic demonstrating the measurement technique is shown in Figure 2. Excitons are selectively photogenerated on specific (*n*,*m*) chiralities of s-SWCNTs by tuning the excitation wavelength into resonance with E_{11} band gap transitions present from 1000 to 1350 nm. The s-SWCNTs can alternatively be excited at their E_{22} transitions (500−700 nm) or at phonon sidebands associated with either the E_{11} or E_{22} transitions. s-SWCNT exciton dissociation and charge transfer are expected when $\Delta EA > E_B$ or $\Delta IP > E_B$, in which ΔEA is the difference between the electron affinity (EA) of the s-SWCNT and the possible electron acceptor and ΔIP is the difference between the ionization potential (IP) of the s-SWCNT and the possible hole acceptor. After their dissociation, the free electronic carriers are able to diffuse away from the interface due to a non-equilibrium concentration gradient, resulting in a charge buildup on the capacitor. The work function offset between the anode and cathode also adds a drift component to the transport, which can be modulated with application of an external bias.

The measured zero-bias, spectrally resolved charging-current photoresponsivity of nanotube/annealed polymer or unannealed fullerene material pairs is shown in Figure 3A. Annealing was observed to improve the photoresponsivity of polymer devices but not fullerene devices. (The unannealed polymer and annealed fullerene nanotube/material pairs are compared in Figure S2, Supporting Information.) Photocurrent responses were observed to be linearly dependent on photon flux, and in the saturation regime of fre-

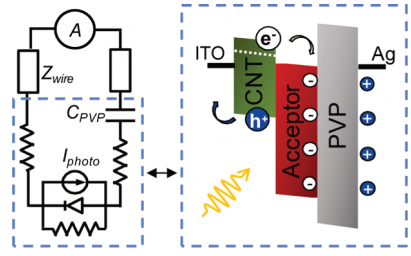

Figure 2. Photosensitive capacitor measurement circuit and energy band diagram. Photogenerated excitons on s-SWCNTs are dissociated at interfaces with acceptors when ΔIP or $\Delta EA > E_B$.

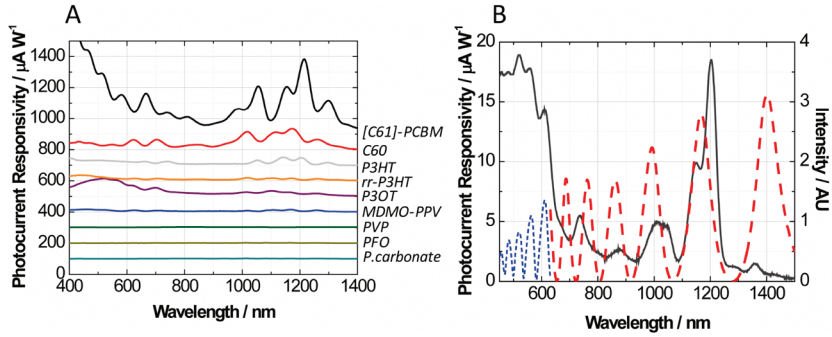

Figure 3. (A) Magnitude of the exciton dissociation driven current responsivity for various 1:1 wt ratio PFO:s-SWCNT/semiconductor heterojunctions measured using photoactive capacitor devices. Responses are offset but not scaled. (B) Responsivity of s-SWCNT/P3OT (black, solid) device compared with calculated, spectrally resolved optical intensity in P3OT (blue, dotted) and in s-SWCNT (red, dashed) for a device stack of glass/ITO (100 nm)/s-SWCNT (7 nm)/P3OT (30 nm)/PVP (1900 nm)/Ag (50 nm).

quency dependence (Figure S3, Supporting Information).

The heterojunctions consisting of s-SWCNTs and fullerene derivatives and s-SWCNTs and poly(thiophene) derivatives demonstrated the largest photoresponsivity (Figure 3A). The spectrally averaged photoresponsivity in the near-infrared (NIR, 900−1400 nm), resulting from excitation of the s-SWCNTs at their E_{11} band gaps, was 58 ± 27, 93 ± 45, 12 ± 3, 5 ± 2, and 11 ± 6 μA W^{-1} ($\bar{x} \pm \sigma$) for s-SWCNTs interfaced with C_{60}, [6,6]-Phenyl C_{61} butyric acid methyl ester ([C61]-PCBM), poly(3-hexylthiophene) (P3HT), regiorandom P3HT (rr-P3HT), and poly(3-octylthiophene) (P3OT), respectively. In the NIR, the measured photoresponse matches the s-SWCNT thin film absorption spectrum (modulated by microcavity effects) indicating that the photoresponsivity arises from excitons originally generated on the s-SWCNTs rather than excitons on the other materials, none of which have significant absorptivity in the NIR. In comparison with the fullerene derivatives and poly(thiophene) derivatives, zero or weak photoresponsivity in the NIR (<1 μA W^{-1}) was observed for s-SWCNT thin films interfaced with polycarbonate, PFO, or a control without a donor or acceptor (referred to as PVP); and a small photoresponse (3 ± 2 μA W^{-1}) was observed for the s-SWCNT/poly(2-methoxy-5-(3′,7′dimethyloctyloxy)-1,4-phenylenevinylene) (MDMO-PPV) sample.

In addition to a signal in the NIR, a photoreponsivity was also observed in response to excitation of the s-SWCNTs at their E_{22} and E_{11} + phonon sideband transitions, from 500 to 800 and 800 to 900 nm, respectively, and in response to optical excitation of the polymeric semiconductor materials in the visible spectrum. The E_{22} + phonon sideband transitions were not resolved due to spectral congestion. Overall, no appreciable spectral broadening was observed in the s-SWCNT photoresponsivity compared with their thin film absorptivity. For example, the full width half max of the photoresponsivity of the (8,6) E_{11} at 1200 nm was 37 ± 11 and 41 ± 6 meV for the poly(thiophene) and fullerene derivative based devices, respectively, compared with 38 ± 5 meV in absorption.

A subset of the E_{11} and E_{22} optical transitions appear missing or suppressed in the photoresponsivity spectra. These suppressed peaks are explained by microcavity effects resulting from spectrally varying interference of the incident and reflected radiation at the heterojunction interface. Small variations in the PVP thickness spectrally shift the interference from substrate to substrate. For instance, decreasing the PVP thickness from 2.0 to 1.95 um shifts a deconstructive interference peak in the E_{11} spectral region from 1144 to 1116 nm. For this reason, interference effects are separately considered for each device. To demonstrate the effects of destructive interference, the optical intensity in a s-SWCNT/P3OT device at the heterointerface has been calculated by using an optical transfer matrix approach with layer thicknesses of 150, 7, 30, 1910, and 50 nm for ITO, s-SWCNT, P3OT, PVP, and Ag, respectively, and is demonstrated in Figure 3B. The absence of strong E_{22} contributions to the photoresponsivity at 655 and 800 nm and the suppressed E_{11} transitions at 1050 and 1280 nm correspond to spectral regions of strong destructive interference in the SWCNT/P3OT photoresponsivity.

An external bias was utilized to determine the polarity of charge transfer for the devices in which s-SWCNT exciton dissociation was observed. From the energy diagram in Figure 1, it is expected that a positive bias applied to the Ag should enhance (inhibit) electron (hole) extraction from the s-SWCNTs resulting in a larger (smaller) photocurrent transient due to the drift component of free carrier transport. The measured effect of the external bias on the responsivity was small (<10% of the overall signal); however, by measuring the direction of the change in responsivity with bias, the charge transfer polarity could be determined. Qualitatively, the measured photoresponsivity of the s-SWCNT/C_{60} and s-SWCNT/[C61]-PCBM photosensitive capacitors increased with the application of a positive bias to the Ag, indicating electron transfer from photoexcited

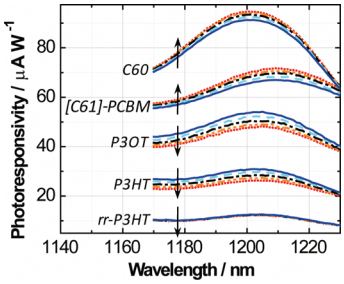

Figure 4. Bias dependent responsivities for s-SWCNTs interfaces with poly(thiophene) derivatives and fullerene derivatives. An arrow denotes the direction of increasing bias (on Ag) from −5 V (solid, blue) to +5 V (dotted, red) in 2.5 V steps. Responsivity curves are offset but not scaled.

s-SWCNTs to the fullerenes (Figure 4). In contrast, the measured photoresponsivity of s-SWCNT/P3HT and s-SWCNT/P3OT photoactive capacitors decreased with the application of a positive bias to the Ag, indicating hole transfer from the s-SWCNTs to the poly(thiophene) derivatives.

The driving force for exciton dissociation and the polarity of charge transfer can be predicted by comparing the energy levels of the s-SWCNTs with the energy levels of the polymeric semiconductor materials, also considering the exciton binding energy. We use the work function calculations of Barone et al.[20] and the exciton binding scaling relationship of Perebeinos et al.[21] with a relative permittivity $\varepsilon_r = 4.0$ to estimate the energetics of the s-SWCNTs. Accordingly, E_B, EA, and IP for the (8,6), (7,6), (7,5), (8,7), and (9,7) chiralities of s-SWCNTs range from 0.2 to 0.26 eV, 3.79 to 3.93 eV, and 5.04 to 5.12 eV, respectively. Therefore, complementary materials with an EA $>$ 4 eV or IP $<$ 4.9 eV should be capable of inducing s-SWCNT exciton dissociation and electron or hole transfer, respectively, for s-SWCNTs in this diameter range. Louie et al.[22] have calculated an EA for C_{60} of 4.05 eV suggesting a $\Delta EA \approx E_B$ (Table 1). Literature values for the IP of the poly(thiophene) derivatives vary from 4.7 to 5.0 eV suggesting a $\Delta IP \approx E_B$. These offsets are thus approximately sufficient for exciton dissociation and are consistent with our observations of electron transfer from the SWCNT to the fullerenes and hole transfer to the poly(thiophene) derivatives.

TABLE 1. Comparison of Measured Photoresponsivity Averaged over the Range 900−1400 nm with Expected Energy Offsets

material	averaged nir Photoresponsivity [μA W^{-1}]	carrier extracted from SWCNT	ionization potential [eV]	electron affinity [eV]
s-SWCNT			3.7−4.1	4.9−5.3
C60[22]	58 ± 27	e^-	6.2	4.0
[C61]-PCBM[29]	93 ± 45	e^-	6.1	3.8
P3HT[24,30,31]	12 ± 3	h^+	4.7	2.1
rr P3HT[24]	5 ± 2	h^+	5.0	2.2
P3OT[32]	11 ± 6	h^+	5.0	2.2
MDMO-PPV[33]	3 ± 2		5.3	2.8
PVP	<1		n/a	n/a
polycarbonate	<1		n/a	n/a
PFO[34]	<1		5.8	2.2

Weak exciton dissociation at the s-SWCNT/MDMO-PPV interface sheds light onto the maximum IP energy level allowable to extract photoexcited holes. An IP = 5.3 eV is expected for MDMO-PPV, which is 0.3−0.5 eV more electronegative than P3HT or P3OT. Accordingly, exciton dissociation and hole transfer from the s-SWCNT to the PPV derivatives should be inhibited by an energy barrier of up to 0.2 eV in addition to E_B. The IP of PFO is even deeper (5.8 eV), further inhibiting exciton dissociation and charge transfer, which is consistent with our results. The wide band gap of poly(carbonate) and poly(vinylpyrrolidone) results in larger energy barriers at the heterojunction interface, inhibiting s-SWCNT exciton dissociation and electron or hole transfer, which is consistent with our measured results.

It is important to note that despite the predictive power of the IP/EA comparisons, the measurement of such energy levels is nontrivial and accompanied by a measurement uncertainty of up to 0.4 eV.[23] Furthermore, quantitative comparison of charge transfer efficiency at the interface between s-SWCNTs and semiconductors is affected by several higher order factors. For example, the IP/EA levels of polymeric electronic materials are highly morphology dependent[24] and will likely be perturbed due to electronic and steric interactions with the s-SWCNTs, as well as surface dipoles and local disruptions in molecular packing. Variation in free carrier extraction efficiency will also have a secondary effect on the measured photoresponsivity and is affected by morphology and crystallinity, which is variable from material to material. For instance, these secondary factors may account for the small difference in the observed photoresponsivity among the different poly(thiophene) derivatives. Nonetheless, while some deviation from the predicted energy offsets is expected, our results are well described by the predicted energy offsets to first order.

The strong exciton dissociation photocurrent measured at the s-SWCNT/C_{60} interface observed here agrees with previous measurements of exciton dissociation at SWCNT/C_{60} interfaces in photodetector devices fabricated by Arnold and Zimmerman et al.[25] Our results also extend beyond that of Arnold and Zimmerman et al.[25] and show that the fullerene derivative [C61]-PCBM and poly(thiophene) derivatives are potential electron and hole acceptors, respectively, that can be paired with s-SWCNTs to achieve the dissociation and separation of photogenerated charges in s-SWCNTs, as well. In particular, these new findings are important because whereas C_{60} is not solution-processable, [C61]-PCBM and the poly(thiophene) derivatives can be dissolved at relatively high concentrations in solvents such as chlorobenzene. As a result, it should be possible to fabricate blended heterojunction devices for photovol-

taic and photodetector applications that will overcome the expected intertube exciton diffusion bottleneck in s-SWCNT thin films.

Previously, Schuettford et al. have indirectly characterized P3HT/s-SWCNT heterojunctions in solution *via* optical spectroscopy of P3HT wrapped SWCNT nanohybrids.[26,11] Specifically, the authors have observed that the E_{11} transitions of s-SWCNTs red-shift when they are wrapped by P3HT in solution. The authors have argued that this red-shift is evidence that the two materials form a type-II heterojunction. While our observation of strong photoresponsivity in P3HT/s-SWCNT thin film heterojunctions supports the type-II heterojunction picture, we have not observed a red-shift of the E_{11} transitions in any of our devices. An in-depth comparison of our findings with those of Schuettford et al. is complicated by the fact that (1) we measure in thin films whereas they measure in solution, (2) we more directly measure the charge transfer whereas they utilize indirect spectroscopic measures, and (3) our s-SWCNT samples are wrapped by PFO, not P3HT. It may be that discrepancies regarding the red-shift result from differences in polarizability in the solid-state versus in solution, or more likely, the partial-monolayer of the PFO wrapper buffering the s-SWCNT/P3HT interface in our samples, which is expected to allow contact between the P3HT and the s-SWCNT but to disrupt the P3HT packing and alter the polarization of the nanotubes.

The lack of an observed charge transfer between photoexcited s-SWCNTs and polycarbonate in our studies conflicts with the findings of Pradhan and coworkers,[17] who have argued that photogenerated excitons on s-SWCNTs dissociate in polycarbonate composites. Our results suggest that the photoconductivity observed by Pradhan et al. may originate from thermal and/or bolometric effects, and not exciton dissociation. Previous measurements with terahertz spectroscopy[27] have suggested that free carriers are generated with >10% efficiency in neat s-SWCNT films even without the implementation of a type-II heterojunction. In contrast with this terahertz spectroscopy work, we do not observe a photoresponse in the absence of a type-II heterojunction. This absence of a response suggests that if photogenerated excitons are dissociated in the bare s-SWCNTs films, the lifetime of resulting free carriers is sufficiently short that these charges rapidly recombine prior to their spatial separation.

CONCLUSION

In conclusion, exciton dissociation and interfacial charge transfer from semiconducting single-walled carbon nanotubes (s-SWCNTs) to a variety of polymeric photovoltaic materials have been studied using a photoactive capacitor measurement technique. It has been shown that photogenerated excitons on s-SWCNTs in thin films are dissociated at interfaces with C_{60}, [C61]-PCBM, P3OT, regioregular and regiorandom P3HT. Photocurrent bias dependencies reveal that fullerene and poly(thiophene) derivatives serve as electron accepting and hole accepting materials to s-SWCNTs, respectively. In contrast, insufficient band offsets for dissociation and charge transfer result when s-SWCNTs are paired with wider gap materials such as MDMO-PPV, PVP, polycarbonate, and PFO. From these results, it is anticipated that photodetector and photovoltaic devices with near-infrared photoresponsivity out to 1350 nm can be fabricated from pairings of P3HT/s-SWCNT, P3OT/s-SWCNT, or s-SWCNT/[C61]-PCBM. Additionally, this work suggests the use of isolated s-SWCNTs as intermediate near-infrared "dyes" in P3HT/[C61]-PCBM blends as a means for achieving broader absorption in polymeric photovoltaic devices. In this case, photogenerated electrons and holes on the s-SWCNTs would transfer to the [C61]-PCBM and P3HT phases, respectively. Beyond the polymeric photovoltaic materials characterized here, it is further anticipated that a host of other materials exist with the appropriate energetics to dissociate excitons on s-SWCNTs, enabling the use of these high-mobility semiconductor absorbers in a wide range of solution-processed photovoltaic and photodetector technologies that are sensitive to a broad spectrum of radiation spanning the visible and infrared.

MATERIALS AND METHODS

s-SWCNT Solutions. HiPCO (1 mg/mL) grown SWCNT (Unidym, raw powder) were sonicated using a horn-tip sonic dismembrator for 45 min in a 10 mg/mL solution of PFO (American Dye Source) in toluene. Bundles and catalyst material were removed through a 1 h centrifugation at 30 000 *g* in a fixed angle rotor (Eppendorf FA-45-24-11-HS.) The supernatant (top 90% of a 3 cm vial) was extracted and centrifuged for 24 h at 30 000 *g*. Over this period, isolated s-SWCNT moved a total distance of 1 cm, accumulating in a "pellet" with >90% yield. The PFO-rich supernatant was removed and discarded. The pellet was redispersed through a low power, horn microtip sonication in toluene, and repelleted in the centrifuge to remove residual free polymer resulting in a pellet with a 4:1 weight ratio of PFO:s-SWCNT. A 1:1 weight ratio of PFO:s-SWCNT was achieved by redispersing the pellet into chlorobenzene and repelleting at 30 130 *g*, resulting in a sedimentation rate of 0.5 cm per 24 h period. The final pellet was redispersed into chloroform to result in a stable, PFO-wrapped s-SWCNT solution.

Photocapacitor Device Fabrication. ITO on glass substrates were first cleaned through a standard degreasing procedure, involving iterative bath sonication in acetone, trichloroethylene, and isopropanol, before 20 min of UV/ozone exposure. Clean ITO-coated substrates and s-SWCNT solutions were then transferred to a nitrogen glovebox where s-SWCNT films were cast *via* doctor-blading at 65 °C with a substrate clearance of 0.2 mm. After deposition, films were then annealed at 130 °C for 1 h to remove excess solvent. Polymer films (PFO, regiorandom P3HT, regioregular-P3HT, and regioregular-P3OT all purchased from ADS, and MDMO-PPV, Polycarbonate, and [C61]-PCBM purchased from Sigma Aldrich) were spun atop CNT films at 1000

rpm from 10 mg/mL solution in chlorobenzene ([C61]-PCBM, 20 mg/mL). A control sample was made by spinning neat chlorobenzene in the same conditions, and was later used to test the PVP/s-SWCNT interface. C_{60} was evaporated from a thermal source (background pressure of 1×10^{-6} Torr), and deposited at a rate of 1.0 Å s^{-1} to a final thickness of 30 nm. A 2 μm film of PVP was spun from a 125 mg mL^{-1} methanol solution at 2000 rpm. Two subsets of active interfaces were fabricated, one subset that was annealed at 130 °C before and after dielectric deposition and one subset that was not annealed at all. Devices were completed with the thermal evaporation of 50 nm silver with a background pressure of 10^{-6} Torr. Absorption spectra were measured after each phase of fabrication and indicate that the s-SWCNT films were robust to the brief presence of chlorobenzene during subsequent spin-casting; therefore, the resulting device architectures are considered planar.

Photocapacitor Characterization. Optical absorption was measured using a home-built setup consisting of a tungsten−halogen light source and a Horiba Jobin Yvon monochromator in conjugation with a modulated 4 kHz chopper wheel and detected using a calibrated Ge reference cell and a Stanford Research Systems SR830 lock-in amplifier. The same setup was modified to measure spectrally resolved responsivity of the photoactive capacitors.

Calculation of Interference Effects. Electromagnetic radiation intensity has been calculated for normal incidence on the given device structure based on work done by Peumans et al.[28] PVP and P3OT thicknesses were measured through standard profilometry techniques (1900 and 30 nm, respectively) and CNT film thickness (7 nm) was approximated through a calculation using absorption data with optical cross section information from Tsyboulski et al.[2]

Acknowledgment. Dominick J. Bindl acknowledges support through a UW-Madison Raymond G. and Anne W. Herb Graduate Fellowship. This work was supported by the National Science Foundation, Grant No. NSF-DMR-0905861.

Supporting Information Available: Figures showing the atomic force micrograph of ITO substrate and s-SWCNT thin film, photocurrent responsivity comparison of photocapacitor devices fabricated without annealing and with annealing, and intensity dependence of measured photocurrent response. This material is available free of charge via the Internet at http://pubs.acs.org.

REFERENCES AND NOTES

1. Kataura, H.; Kumazawa, Y.; Maniwa, Y.; Umezu, I.; Suzuki, S.; Ohtsuka, Y.; Achiba, Y. Optical Properties of Single-Wall Carbon Nanotubes. *Synth. Met.* **1999**, *103*, 2555–2558.
2. Tsyboulski, D. A.; Rocha, J. D. R.; Bachilo, S. M.; Cognet, L.; Weisman, R. B. Structure-Dependent Fluorescence Efficiencies of Individual Single-Walled Carbon Nanotubes. *Nano Lett.* **2007**, *7*, 3080–3085.
3. Durkop, T.; Getty, S. A.; Cobas, E.; Fuhrer, M. S. Extraordinary Mobility in Semiconducting Carbon Nanotubes. *Nano Lett.* **2004**, *4*, 35–39.
4. Avouris, P.; Martel, R. Progress in Carbon Nanotube Electronics and Photonics. *MRS Bull.* **2010**, *35*, 306–313.
5. Gabor, N. M.; Zhong, Z. H.; Bosnick, K.; Park, J.; McEuen, P. L. Extremely Efficient Multiple Electron-Hole Pair Generation in Carbon Nanotube Photodiodes. *Science* **2009**, *325*, 1367–1371.
6. Liu, J.; Hersam, M. C. Recent Developments in Carbon Nanotube Sorting and Selective Growth. *MRS Bull.* **2010**, *35*, 315–321.
7. Wang, F.; Dukovic, G.; Brus, L. E.; Heinz, T. F. The Optical Resonances in Carbon Nanotubes Arise from Excitons. *Science* **2005**, *308*, 838–841.
8. Freitag, M.; Martin, Y.; Misewich, J. A.; Martel, R.; Avouris, P. H. Photoconductivity of Single Carbon Nanotubes. *Nano Lett.* **2003**, *3*, 1067–1071.
9. Lee, J. U., Photovoltaic Effect in Ideal Carbon Nanotube Diodes. *Appl. Phys. Lett.* **2005**, *87*, 1−3.
10. Wang, S.; Zhang, L. H.; Zhang, Z. Y.; Ding, L.; Zeng, Q. S.; Wang, Z. X.; Liang, X. L.; Gao, M.; Shen, J.; et al. Photovoltaic Effects in Asymmetrically Contacted CNT Barrier-Free Bipolar Diode. *J. Phys. Chem. C* **2009**, *113*, 6891–6893.
11. Schuettfort, T.; Nish, A.; Nicholas, R. J. Observation of a Type II Heterojunction in a Highly Ordered Polymer-Carbon Nanotube Nanohybrid Structure. *Nano Lett.* **2009**, *9*, 3871–3876.
12. St-Antoine, B. C.; Menard, D.; Martel, R. Position Sensitive Photothermoelectric Effect in Suspended Single-Walled Carbon Nanotube Films. *Nano Lett.* **2009**, *9*, 3503–3508.
13. Avouris, P.; Freitag, M.; Perebeinos, V. Carbon-Nanotube Photonics and Optoelectronics. *Nat. Photonics* **2008**, *2*, 341–350.
14. Kanai, Y.; Grossman, J. C. Role of Semiconducting and Metallic Tubes in P3HT/Carbon-Nanotube Photovoltaic Heterojunctions: Density Functional Theory Calculations. *Nano Lett.* **2008**, *8*, 908–912.
15. Kazaoui, S.; Minami, N.; Nalini, B.; Kim, Y.; Hara, K. Near-Infrared Photoconductive and Photovoltaic Devices Using Single-Wall Carbon Nanotubes in Conductive Polymer Films. *J. Appl. Phys.* **2005**, *98*, 1−6.
16. Kymakis, E.; Amaratunga, G. A. J. Carbon Nanotubes as Electron Acceptors in Polymeric Photovoltaics. *Rev. Adv. Mater. Sci.* **2005**, *10*, 300–305.
17. Pradhan, B.; Setyowati, K.; Liu, H. Y.; Waldeck, D. H.; Chen, J. Carbon Nanotube - Polymer Nanocomposite Infrared Sensor. *Nano Lett.* **2008**, *8*, 1142–1146.
18. Nish, A.; Hwang, J. Y.; Doig, J.; Nicholas, R. J. Highly Selective Dispersion of Singlewalled Carbon Nanotubes Using Aromatic Polymers. *Nat. Nanotechnol.* **2007**, *2*, 640–646.
19. Bachilo, S. M.; Strano, M. S.; Kittrell, C.; Hauge, R. H.; Smalley, R. E.; Weisman, R. B. Structure-Assigned Optical Spectra of Single-Walled Carbon Nanotubes. *Science* **2002**, *298*, 2361–2366.
20. Barone, V.; Peralta, J. E.; Uddin, J.; Scuseria, G. E. Screened Exchange Hybrid Density-Functional Study of the Work Function of Pristine and Doped Single-Walled Carbon Nanotubes. *J. Chem. Phys.* **2006**, *124*, 5.
21. Perebeinos, V.; Tersoff, J.; Avouris, P. Scaling of Excitons in Carbon Nanotubes. *Phys. Rev. Lett.* **2004**, *92*, 257402.
22. Shirley, E. L.; Louie, S. G. Electron Excitations in Solid C-60 - Energy-Gap, Band Dispersions, and Effects of Orientational Disorder. *Phys. Rev. Lett.* **1993**, *71*, 133–136.
23. Helander, M. G.; Greiner, M. T.; Wang, Z. B.; Lu, Z. H. Pitfalls in Measuring Work Function Using Photoelectron Spectroscopy. *Appl. Surf. Sci.* **2010**, *256*, 2602–2605.
24. Kanai, K.; Miyazaki, T.; Suzuki, H.; Inaba, M.; Ouchi, Y.; Seki, K. Effect of Annealing on the Electronic Structure of poly(3-hexylthiophene) Thin Film. *Phys. Chem. Chem. Phys.* **2010**, *12*, 273–82.
25. Arnold, M. S.; Zimmerman, J. D.; Renshaw, C. K.; Xu, X.; Lunt, R. R.; Austin, C. M.; Forrest, S. R. Broad Spectral Response Using Carbon Nanotube/Organic Semiconductor/C-60 Photodetectors. *Nano Lett.* **2009**, *9*, 3354–3358.
26. Schuettfort, T.; Snaith, H. J.; Nish, A.; Nicholas, R. J. Synthesis and Spectroscopic Characterization of Solution Processable Highly Ordered Polythiophene-Carbon Nanotube Nanohybrid Structures. *Nanotechnology* **2000**, *21*, 9.
27. Beard, M. C.; Blackburn, J. L.; Heben, M. J. Photogenerated Free Carrier Dynamics in Metal and Semiconductor Single-Walled Carbon Nanotube Films. *Nano Lett.* **2008**, *8*, 4238–4242.
28. Peumans, P.; Yakimov, A.; Forrest, S. R. Small Molecular Weight Organic Thin-Film Photodetectors and Solar Cells. *J. Appl. Phys.* **2003**, *93*, 3693–3723.
29. Koster, L. J. A.; Mihailetchi, V. D.; Blom, P. W. M. Ultimate Efficiency of Polymer/Fullerene Bulk Heterojunction Solar Cells. *Appl. Phys. Lett.* **2006**, *88*, 3.
30. Cascio, A. J.; Lyon, J. E.; Beerbom, M. M.; Schlaf, R.; Zhu, Y.; Jenekhe, S. A. Investigation of a Polythiophene Interface Using Photoemission Spectroscopy in Combination with

Electrospray Thin-Film Deposition. *Appl. Phys. Lett.* **2006**, *88*, 3.
31. Sohn, Y.; Stuckless, J. T. Characteristics of Photoexcitations and Interfacial Energy Levels of Regioregular poly(3-hexythiophene-2,5-diyl) on Gold. *ChemPhysChem* **2007**, *8*, 1937–1942.
32. Wagner, J.; Pielichowski, J.; Hinsch, A.; Pielichowski, K.; Bogdal, D.; Pajda, M.; Kurek, S. S.; Burczyk, A. New Carbazole-Based Polymers for Dye Solar Cells with Hole-Conducting Polymer. *Synth. Met.* **2004**, *146*, 159–165.
33. Beek, W. J. E.; Wienk, M. M.; Janssen, R. A. J. Efficient Hybrid Solar Cells from Zinc Oxide Nanoparticles and a Conjugated Polymer. *Adv. Mater.* **2004**, *16*, 1009.
34. Gong, X.; Moses, D.; Heeger, A. J.; Xiao, S. Excitation Energy Transfer from Polyfluorene to Fluorenone Defects. *Synth. Met.* **2004**, *141*, 17–20.